

Received: 2018.09.04
Accepted: 2018.10.10
Published: 2019.01.30

Overexpression of E74-Like Factor 5 (ELF5) Inhibits Migration and Invasion of Ovarian Cancer Cells

Authors' Contribution:
Study Design A
Data Collection B
Statistical Analysis C
Data Interpretation D
Manuscript Preparation E
Literature Search F
Funds Collection G

ABE 1 Xiaofeng Zhang
BEF 1 Jing Lin
CEF 2 Yanping Ma
CDE 3 Jiali Zhao

1 Department of Gynecology, Chengyang People's Hospital, Qingdao, Shandong, P.R. China
2 Department of Geriatrics, Chengyang People's Hospital, Qingdao, Shandong, P.R. China
3 Department of Gynecology, Dezhou Women's and Children's Hospital, Qingdao, Shandong, P.R. China

Corresponding Author: Jiali Zhao, e-mail: zhaojiali_jlzhao@163.com
Source of support: Departmental sources

Background: E74-like factor 5 (ELF5) plays a key role in the processes of cell differentiation, apoptosis, and occurrence of tumors. However, the effect of ELF5 on metastasis and invasion in human ovarian cancer remains poorly understood.

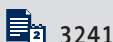
Material/Methods: Quantitative real-time polymerase chain reaction (qPCR) was performed to measure the expression of ELF5. The viability of cells was detected by cell counting kit (CCK-8). Cell apoptosis was tested by flow cytometry. Matrigel plug angiogenesis assay was employed to determine angiogenesis rate. The protein expression levels of vascular endothelial growth factor (VEGF), cleaved caspase-3, B-cell lymphoma 2 (Bcl-2), Bcl-2-associated X protein (Bax), E-cadherin, N-cadherin, Snail, phosphoinositide 3 kinase (PI3K), phosphorylated (p)-PI3K, tyrosine kinase B (AKT), and phosphorylated (p)-AKT were determined by Western blot. Wound-healing assay and Transwell were used to determine invasion and migration.

Results: We found that expression of ELF5 was obviously decreased in ovarian cancer cell lines. The cells viability, invasion and metastasis were inhibited by overexpression ELF5. ELF5 suppressed angiogenesis rate and the expression of VEGF. Changes of the expressions of Bcl-2, cleaved caspase-3 and Bax showed that anti-apoptosis ability was improved by ELF5. ELF5 also repressed N-cadherin and Snail and increased E-cadherin. The expressions of p-PI3K and p-AKT were decreased by ELF5. Further study showed that IGF-I reversed the inhibitory effect of ELF5 on growth and metastasis of SKOV3 cells.

Conclusions: Overexpression of ELF5 promoted the apoptosis and reduced the migration and invasion of ovarian cancer cells; therefore, it could provide a new approach to gene treatment of ovarian carcinoma.

MeSH Keywords: Ephrin-A2 • Neoplasm Invasiveness • Neoplasm Metastasis • Ovarian Neoplasms

Full-text PDF: <https://www.medscimonit.com/abstract/index/idArt/913058>



Background

Ovarian malignant tumor is one of the gynecological malignant tumors that threaten women's health [1]. Ovarian malignant tumor is more common in ovarian epithelial cancer, and the mortality rate is the highest in gynecological malignant tumors [1,2]. The disease is difficult to diagnose at an early stage, and the treatment outcome of ovarian cancer is usually poor [3]. Therefore, it is necessary to study and elucidate the specific mechanism of ovarian cancer invasion and metastasis, and to design corresponding treatment strategies in a targeted manner that can improve clinical therapeutic outcome of treating ovarian cancer as well as patients' survival rates [4,5].

E74-like factor 5 (ELF5) is an epithelial-specific member of the Ets transcription factor family, which plays a crucial role in cell differentiation and apoptosis, and tissue formation, and is a long-term regulator of tumor cell proliferation [6]. Recent studies have shown that ELF5 is not only a cell home regulator, but also an EMT tumor suppressor, as it inhibits Snail transcription and the progression of EMT [7].

The concept of epithelial-mesenchymal transition (EMT) was proposed in the 1980s [8]. It is an epithelial cell that loses normal polarity of cells and tight junctions among cells, and differentiates mesenchymal cells. Epithelial cells often lose their cell polarity and obtain higher interstitial phenotypes such as invasion and migration [9,10]. The main features of EMT are decreased expression of cell adhesion molecules such as E-cadherin, increased expression of interstitial adhesion molecules such as N-cadherin, and conversion of the cyokeratin skeleton to vimentin-based cytoskeleton, as well as some other features such as morphological differentiation with mesenchymal cells [8]. Studies have shown that activation of signal transduction pathways such as PI3K/AKT can promote the development of EMT and the migration and metastasis of tumor cells [11].

It has been found that overexpression of PI3K in ovarian cells is an important factor for the transformation of normal ovarian cells into poorly differentiated and highly proliferating malignant cells [12]. PI3K is essential in the process of growth factor superfamily regulating signal transduction molecules. Various cytokines and physical and chemical factors are activated, and AKT is mainly responsible for the transmission of biological information initiated by P13K [13]. As a main signaling pathway, PI3K/AKT plays a vital role in many biological processes such as cell metabolism, cell cycle regulation, and apoptosis [14].

Therefore, we conducted an in-depth study of ELF5 to elucidate its molecular role in the progression and metastasis of ovarian cancer, and to provide a theoretical basis and clinical guidance for the treatment of ovarian cancer.

Material and Methods

Cells and drugs

Human ovarian cancer cell lines A2780, SKOV-3, ES-2, and OVCAR3 were purchased from the American Type Culture Collection (ATCC; Rockville, MD, USA). HO8910, 3AO, HEY, and NOEC were obtained from Shanghai. Transfection reagent Lipofectamine™ 3000 was purchased from Invitrogen (Thermo Fisher Scientific, Inc.). CCK-8 assay kits were obtained from Nanjing Jiancheng Bioengineering Institute (Nanjing, China).

Cell culture and transfection

Human ovarian cancer cell lines (A2780, SKOV-3, ES-2, OVCAR3, HO8910, 3AO, and HEY) and human normal ovarian epithelial cells (NOEC) were cultured in Roswell Park Memorial Institute (RPMI) 1640 medium containing 10% (v/v) fetal bovine serum (FBS), 10 mmol/L hydroxyethyl piperazine ethanesulfonic acid, 2 mmol/L L-glutamine, 50 μmol/L β-mercaptoethanol, 1 μmol/L sodium pyruvate, 10 μg/mL streptomycin, and 100 U/mL penicillin (Gibco, New York, NY, U.S.A.) at 37°C in a humidified atmosphere of 5% CO₂. Lipofectamine™ 3000 (Thermo Fisher Scientific, Inc.) was used according to the manufacturer's instructions. In brief, the lipid complex was prepared by combining the reagent of 4 μl LFN Plus with 2 μg of plasmid DNA suspended in 1 ml of serum-free medium and incubated at room temperature for 15 min. The solution was then mixed with 40 μl LFN in 1 ml serum-free medium and incubated further at room temperature for 15 min. Lipid compounds were diluted in serum-free medium to produce a volume of 5 ml at the required concentration, and incubated with SKOV-3 cells (8×10⁴/well) in an incubator with 5% CO₂ at 37°C for 24 h for subsequent experimentation.

Cell viability assay

After the SKOV-3 cells were transfected, 10 μl of CCK-8 solution was added to the wells at 12, 24, and 48 h post-culture, and the cells were incubated at 37°C for 2 h in an incubator with 5% CO₂ in the dark. Subsequently, the OD of each well in different cell groups at an absorbance of 450 nm was read by a microplate reader (Bio-Rad Laboratories, Inc., Hercules, CA, USA). Cell viability was detected by CCK-8 assay kit according to the manufacturer's protocol.

Wound-healing assay

After the SKOV-3 cells were transfected for 24 h, a straight gap was created by a 200 μl sterile tip in the middle of the well. The cells were washed by DMEM 2 times for smoothing the edges of the scratch and removing floating cells. After being incubated in an incubator (37°C, 5% CO₂) for 0 h and 24 h, the migration images of the cells were observed under a microscope

(Keyence, Osaka, Japan). The distance of cell migration was visualized and images were taken using image-Pro Plus Analysis software (Media Cybernetics Company, USA).

Transwell

An 8- μm Transwell chamber (3413, American Corning Company, New York, USA) was placed on a 24-well plate with a layer of 50 μl Matrigel (BD, Biosciences) coated on the Transwell chamber. The SKOV-3 cells were cultured in serum-free medium for 12 h to eliminate the effects of the serum, and then resuspended in DMEM that contained bovine serum albumin (BSA; Sigma-Aldrich Chemical Company, St Louis MO, USA) with free FBS. We added 100 μl of the suspended cells to the Transwell chamber, and 400 μl of DMEM containing 20% FBS was added to the basolateral chamber. The cells were cultured for 24 h at 37°C in an incubator with 5% CO_2 . Next, cells collected from the lower chamber were fixed in methanol solution for 30 min and stained with 0.1% crystal violet for 20 min at room temperature. The chamber was washed several times with PBS, and the upper chamber liquid was aspirated. The unigrated cells in the upper layer were gently wiped off using a cotton swab. The membrane was then transferred to a glass slide and sealed with a neutral gum. Images were observed and collected using an inverted optical microscope (Keyence, Osaka, Japan).

In vitro angiogenesis experiment

Matrigel plug angiogenesis assay (Corning, NY, USA) was used to evaluate the *in vitro* anti-angiogenic effect of ELF5. The Matrigel stock solution was thawed overnight at 4°C. A gel solution was prepared using a Matrigel stock solution and serum-free RPMI-1640 medium, and the solution was placed in a 96-well plate and then allowed to incubate for 2 h to cure. The cultured SKOV-3 cells were collected and digested to prepare a single-cell suspension under aseptic conditions, and the cell suspension was adjusted to a density of $1 \times 10^5/\text{ml}$. The cells were seeded in 96-well plates at 100 μl per well. The plates were incubated for 6–8 h in an incubator (5% CO_2 , 37°C), and the cells were visualized using an inverted microscope (Thermo Fisher Scientific) and photographed.

Cell apoptosis

SKOV-3 cells ($1.3 \times 10^5/\text{well}$) were seeded in 6-well plates, after the cells were treated, the supernatant was collected into a 15-ml centrifuge tube, and the culture flask was gently washed once by adding 2 ml of phosphate buffer saline (PBS). The cells were digested with trypsin (1 ml) without ethylenediaminetetraacetic acid (EDTA) and shaken gently. The pancreatic enzyme was aspirated after the wall became wet. The mixture was allowed to stand at room temperature for 1 min, and Dulbecco's modified Eagle medium (DMEM, Corning) containing 10% fetal

bovine serum (FBS, Gibco) was then added to terminate the digestion. The cells were centrifuged at $1000 \times g$ for 3 min and the supernatant was removed. The cells were washed twice with pre-cooled PBS and resuspended in 1X Annexin V binding buffer. According to the Annexin-V-FITC cell apoptosis detection kit (K201-100, BioVision, Milpitas, CA, USA), cells were collected and stained with Annexin V-FITC and propidium iodide (PI) at room temperature for 15 min and counted by flow cytometry (version 10.0, FlowJo, FACS CaliburTM, BD, Franklin Lakes, NJ, USA). Flow cytometry scatter diagrams showed that living cells were in the lower left quadrant, and were mechanically damaged, or that necrotic cells were in the left upper quadrant and necrotic. While advanced apoptotic cells were in the upper right quadrant, the early apoptotic cells were in the lower right quadrant.

Western blot

SKOV-3 cells were washed with PBS twice, and added to protein lysis buffer (RIPA; Cell Signaling Technology, Inc., Danvers, MA, USA) on ice for 2 h. The cells were centrifuged at $12\,000 \times g$ for 30 min at 4°C, and then supernatant was collected. The protein concentration was tested using the BCA protein kit (Bio-Rad Laboratories, Inc., Hercules, CA, USA). We electrophoresed 30- μg samples using 10% SDS-PAGE gels. The gels were transferred to polyvinylidene fluoride membranes (PVDF; Bio-Rad Laboratories, Inc., Hercules, CA, USA) on ice for 110 min at 110 V. The membranes were blocked with 5% BSA (Gibco, USA) and eluted 3 times with TBS for 5 min. The bands were then incubated overnight with the corresponding primary antibody at 4°C. Next, the bands were incubated with secondary antibody horseradish peroxidase (HRP)-conjugated goat anti-mouse/rabbit IgG (1: 2000; sc-516102/sc-2357; Santa Cruz Biotechnology, Inc., Dallas, TX, USA) for 2 h at room temperature. The development was carried out with a developer (EZ-ECL kit; Biological Industries BI), and the gray value of the strips were analyzed and counted using ImageJ software (version 5.0; Bio-Rad, Hercules, CA, USA). The antibodies used in the present study were as follows: anti-GAPDH (mouse; 1: 1000; sc-47724; Santa Cruz Biotechnology), anti-cleaved caspase-3 (mouse; 1: 1000; ab13585; Abcam), anti-VEGF (rabbit; 1: 1000; #2463; CST), anti-E-cadherin (mouse; 1: 1000; ab1416; Abcam), anti-N-cadherin (rabbit; 1: 1000; ab18203; Abcam), anti-Snail (goat; 1: 1000; ab53519; Abcam), anti-Bcl-2 (rabbit; 1: 1000; ab32124; Abcam), anti-Bax (rabbit; 1: 1000; ab32503; Abcam), anti-PI3K (rabbit; 1: 1000; ab151549; Abcam), anti-p-PI3K (rabbit; 1: 1000; ab182651; Abcam), anti-AKT (rabbit; 1: 1000; ab8805; Abcam), and anti-p-AKT (rabbit; 1: 1000; ab38449; Abcam).

RNA isolation and real-time PCR

The cell culture medium in each well was aspirated as much as possible, and 1 ml of Trizol (Invitrogen, Carlsbad, California) was added to the SKOV-3 cells. The cells were placed horizontally for a while and blown evenly. The cells containing the lysate were transferred

Table 1. The primer sequences used for qRT-PCR analysis.

Genes	Forward	Reverse
ELF5	5'-GATCTGTTTCAGCAATGAAG-3'	5'-GGTCTCTTCAGCATCATTG-3'
E-cadherin	5'-AAGGCACAGCCTGTCGAAGCA-3'	5'-ACGTTGTCCCGGGTGCATCCT-3'
N-cadherin	5'-AGGGTGGACGTCATTGTAGC-3'	5'-CTGTTGGGGTCTGTCAGGAT-3'
Snail	5'-CTCCAGCAGCCCTACGAC-3'	5'-CGGTGGGGTTGAGGATCT-3'
GAPDH	5'-ACTTTGGTATCGTGAAGGACTCAT-3'	5'-GTTTTTCTAGACGGCAGGTCAGG-3'

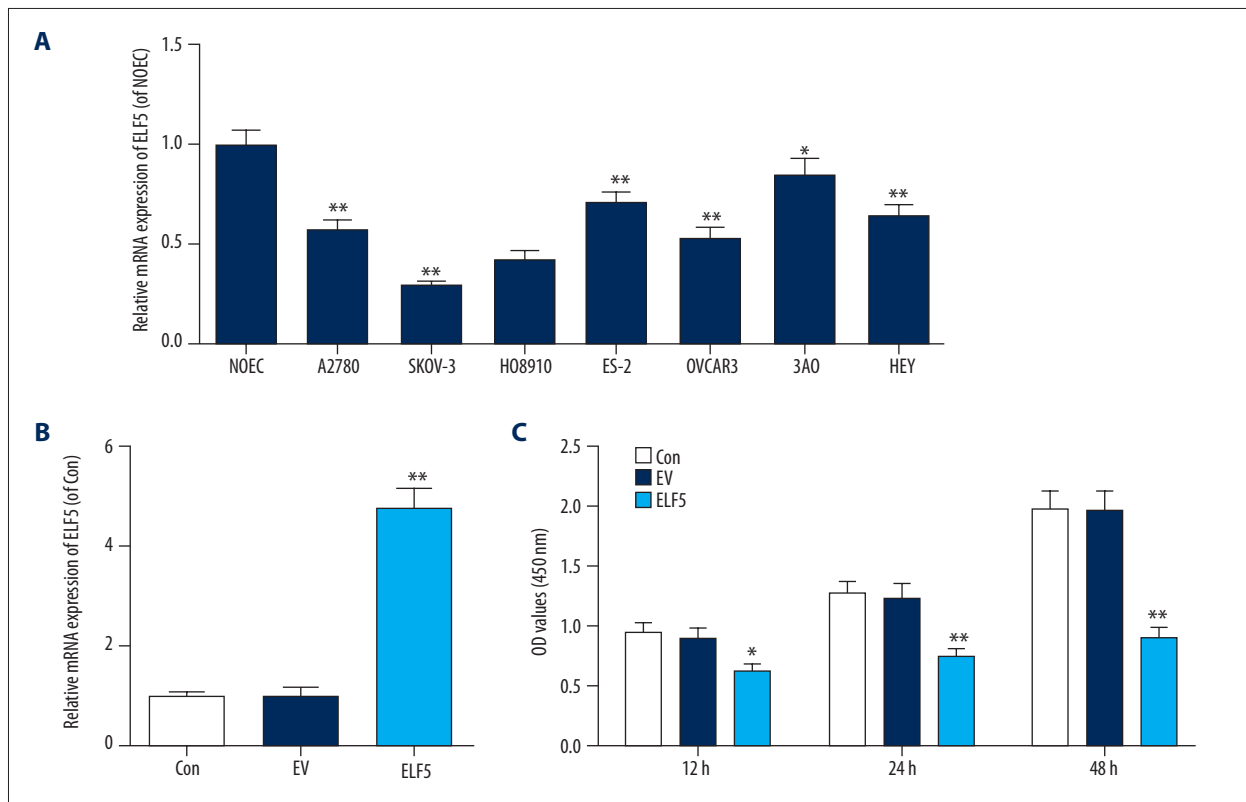


Figure 1. E74-like factor 5 (ELF5) was low expression in ovarian cancer cell lines. (A) E74-like factor 5 (ELF5) was low expression in SKOV-3. (B) Quantitative real-time polymerase chain reaction (qPCR) was used to determine the efficiency of E74-like factor 5 (ELF5) transfection. (C) The viability of cell was decreased by E74-like factor 5 (ELF5). All data were shown as means \pm SEM. * $P < 0.05$, ** $P < 0.01$, vs. control.

to a 1.5-ml EP tube and allowed to stand at room temperature for 5 min. We added 200 μ l of chloroform into each tube and inverted it for 15 s. After being centrifuged at 12 000 \times g for 15 min at 4 $^{\circ}$ C, the upper aqueous phase was pipetted into a new 1.5 ml of EP, and an equal volume of isopropanol (about 400 μ l) was added into each tube and allowed to stand at room temperature for 10 min. After being centrifuged at 12 000 \times g for 15 min at 4 $^{\circ}$ C, the supernatant was discarded and 1 ml of pre-cooled 75% ice-cold ethanol was added. The supernatant was discarded after being centrifuged at 7500 \times g for 10 min at 4 $^{\circ}$ C. An appropriate amount of DEPC (20 μ l) was added to dissolve the RNA. The purity and concentration of RNA was tested by 260 nm/280 nm using the NanoDrop nd – 1000

spectrophotometer (NanoDrop Technologies, Wilmington, DE, USA). According to the program provided by the manufacturer (Thermo Fisher Scientific, Waltham, USA), reverse transcription cDNA kit was used to reverse transcribe 1 microgram total RNA for Synthesis of cDNA (at 42 $^{\circ}$ C for 60 min, at 70 $^{\circ}$ C for 5 min, and preservation at 4 $^{\circ}$ C). SYBR Green PCR Master Mix (Roche, Basle, Switzerland) was used to perform a quantitative real-time polymerase chain reaction (qPCR) experiment using the Opticon real-time PCR Detection System (ABI 7500, Life technology, USA), and the PCR cycle was as follows: a pretreatment at 95 $^{\circ}$ C for 10 min; followed by 40 cycles at 94 $^{\circ}$ C for 15 s, at 60 $^{\circ}$ C for 1 min, and finally at 60 $^{\circ}$ C for 1 min and at 4 $^{\circ}$ C for preservation. The relative mRNA quantity was determined

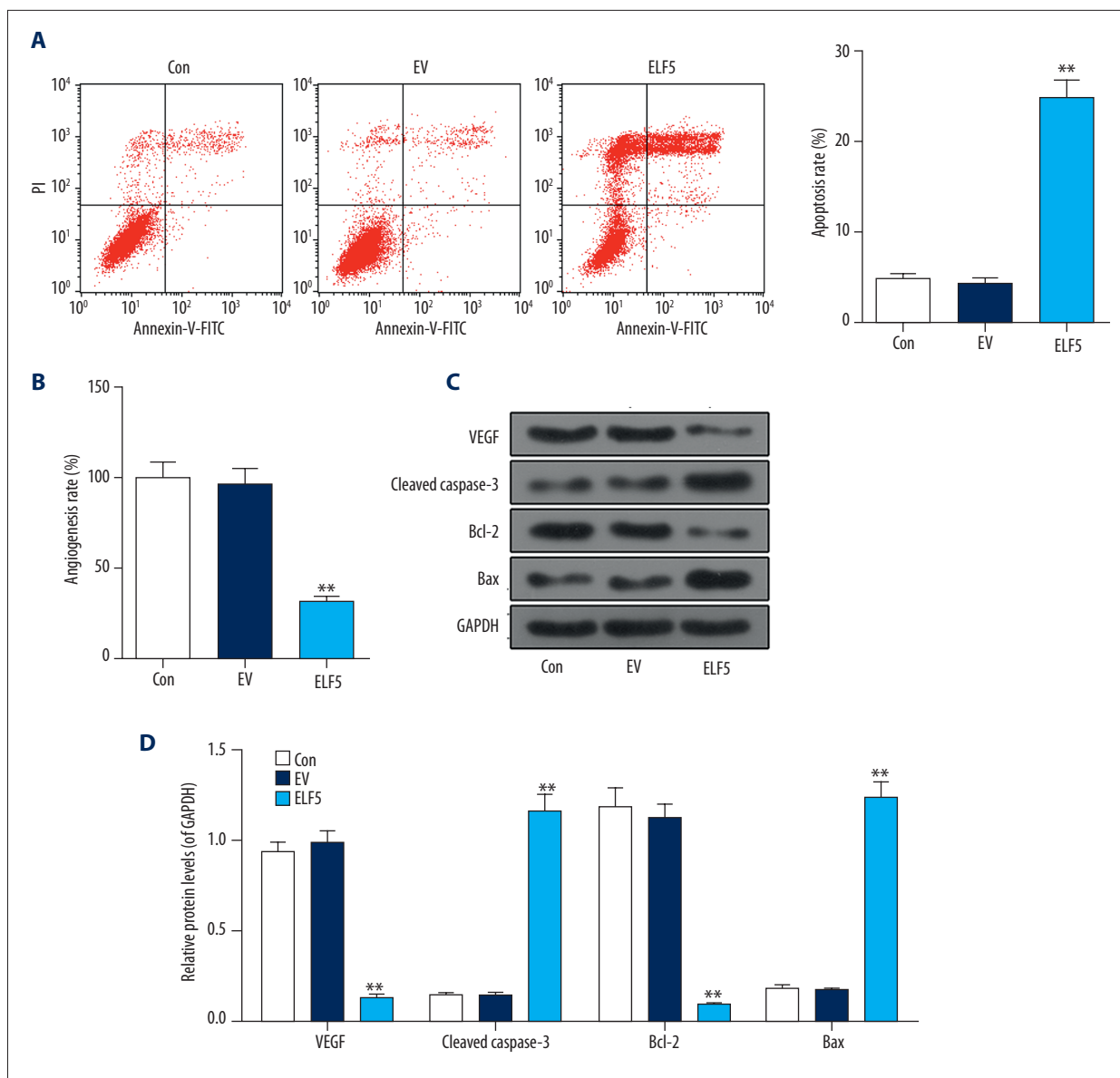


Figure 2. Apoptosis was increased and angiogenesis was attenuated by E74-like factor 5 (ELF5). **(A)** Flow cytometry is used to detect apoptosis. **(B)** *In vitro* vascular experiments were performed to detect angiogenesis. **(C, D)** Western blot analysis showed the effect of E74-like factor 5 (ELF5) on the expression of vascular endothelial growth factor (VEGF), cleaved caspase-3, Bcl-2 and Bax. All data were shown as means \pm SEM. ** $P < 0.01$, vs. control.

using the comparative cycle threshold ($\Delta\Delta Ct$) method [15]. GAPDH expression was used for normalization. The primer sequences used for qRT-PCR analysis are listed as Table 1.

Results

Low expression of ELF5 in ovarian cancer cell lines

To select a suitable ovarian cancer cell line, qPCR was performed to determine the expression of ELF5 in ovarian cancer cell lines.

We discovered that ELF5 was downregulated in ovarian cancer cell lines, especially in SKOV-3 (Figure 1A). Thus, SKOV-3 cell was selected for subsequent experiments. The efficiency of STC2 transfection was tested by qPCR, and we found that ELF5 was overexpressed by plasmid transfection (Figure 1B), and that the viability of cells was attenuated by ELF5 (Figure 1C).

ELF5 increased apoptosis and inhibited angiogenesis

We investigated the effect of overexpression ELF5 on ovarian cancer, and found that apoptosis was increased by ELF5

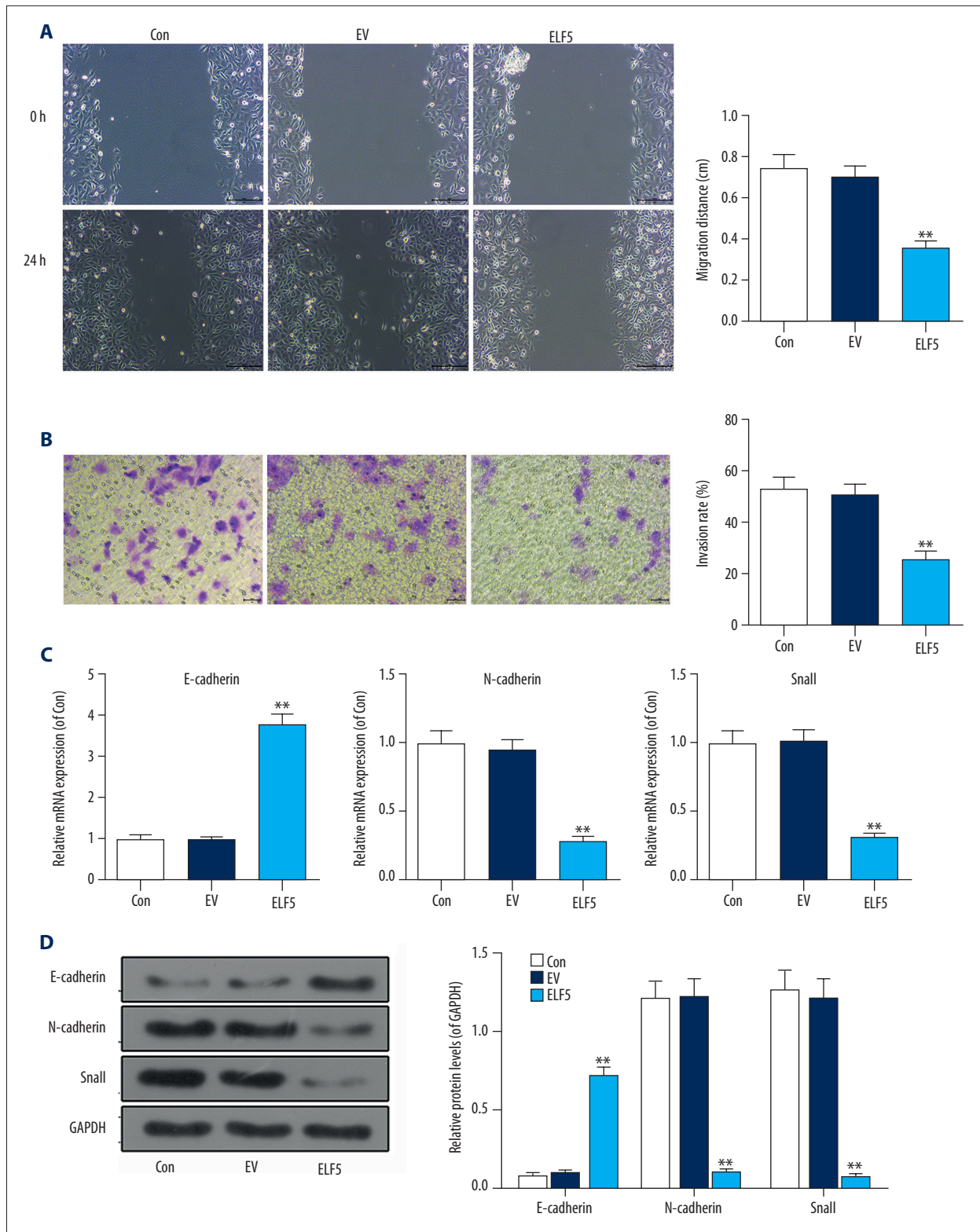


Figure 3. E74-like factor 5 (ELF5) inhibited the migration and invasion. **(A)** The wound assay was used to perform the migration. **(B)** Transwell assay was used to test the invasion. **(C)** The mRNA levels of E-cadherin, N-cadherin and Snail were determined by quantitative real-time polymerase chain reaction (qPCR). **(D)** The protein levels of E-cadherin, N-cadherin and Snail were tested by Western blot. All data were shown as means \pm SEM. ** $P < 0.01$, vs. control.

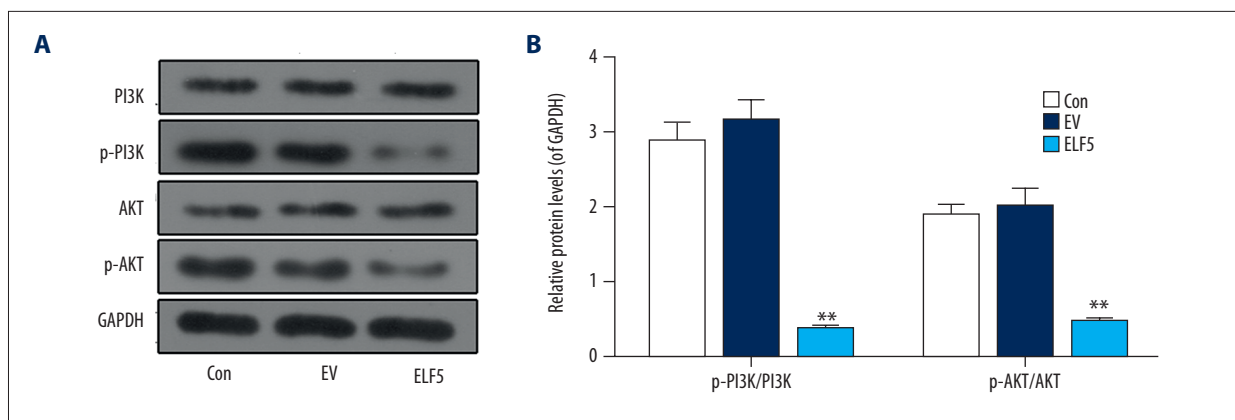


Figure 4. The protein levels of phosphoinositide 3 kinase (PI3K) and tyrosine kinase B (AKT) were repressed by E74-like factor 5 (ELF5). (A, B) Western blot was used to determine the protein levels of phosphoinositide 3 kinase (PI3K) and tyrosine kinase B (AKT). All data were shown as means \pm SEM. ** $P < 0.01$, vs. control.

(Figure 2A), and that the angiogenesis rate was inhibited by ELF5 (Figure 2B). ELF5 downregulated the protein levels of VEGF and Bcl-2 and upregulated cleaved caspase-3 and Bax (Figure 2C).

The invasion and migration were suppressed by ELF5

We discovered that the migration (Figure 3A) and invasion (Figure 3B) were inhibited by ELF5. Compared with control or EV group, the mRNA level of E-cadherin was increased, while the mRNA levels of N-cadherin and Snail were decreased in the ELF5 group (Figure 3C). Similarly, the protein level of E-cadherin was also improved; however, the protein levels of N-cadherin and Snail were decreased by ELF5 (Figure 3D).

The protein levels of p-PI3K and p-AKT were repressed by ELF5

Studies have reported that the PI3K/AKT signaling pathway is involved in the development of ovarian cancer [16]. In this study, Western blot was carried out to test the levels of PI3K and AKT, and we found ELF5 significantly inhibited the expressions of PI3K and AKT (Figure 4A, 4B).

IGF-I reversed the inhibitory effect of ELF5 on growth and metastasis of SKOV3 cells

We treated SKOV-3 cells with PI3K/AKT agonist IGF-1 (100 ng/ml). The migration (Figure 5A) and invasion (Figure 5B) were stronger in the ELF5+IGF-1 group than in the ELF5 group. The proportion of cell invasion and migration are described in Figure 5C, 5D. Compared with the ELF5 group, the viability of cells was increased by IGF-1 (Figure 4E).

Discussion

Ovarian cancer is the second most common female reproductive malignancy, and its mortality rate ranks first among gynecological tumors [17]. Approximately 200 000 people are diagnosed with ovarian cancer each year worldwide, and 125 000 people die of this disease annually [18]. Studies have shown that ELF5 is involved in the development of ovarian cancer [19,20]. However, its mechanism is not fully understood. Therefore, this study explored the mechanism of ELF5 in ovarian cancer.

To further investigate ELF5, we constructed a recombinant plasmid to overexpress ELF5 on SKOV3 cells, and QPCR experiments confirmed that ELF5 was successfully transfected at the mRNA level. Subsequently, the effect of ELF5 gene transfection on the biological behavior of ovarian cancer SKOV3 cells were studied *in vitro*. One of the most important features of tumor cells is cell proliferation, which can be indicated by cell viability [21,22]. Herein, the viability of SKOV3 cells, a pivotal indicator of cell survival, was significantly reduced by overexpression of ELF5, suggesting that ELF5 expression delayed the proliferation of ovarian cancer SKOV3 cells.

Chemotherapy of malignant tumors relies mainly on apoptosis of tumor cells in order to fulfill therapeutic purposes [23,24], and by regulating the balance of cell growth and death, apoptosis is crucial in maintaining balance in the body [22]. ELF5 inhibits the proliferation of cancer cells by inducing apoptosis [25,26]. Therefore, most cancer therapeutic drugs function via the apoptotic pathway. Apoptotic proteins such as cleaved caspase-3, Bax, and Bcl-2 play important roles in the apoptotic pathway [27]. We found that the apoptosis rate of ovarian cancer SKOV3 cells was significantly increased after ELF5 gene transfection, while the expressions of pro-apoptotic proteins cleaved caspase-3 and Bax increased, and that the expression of anti-apoptotic protein Bcl-2 was downregulated.

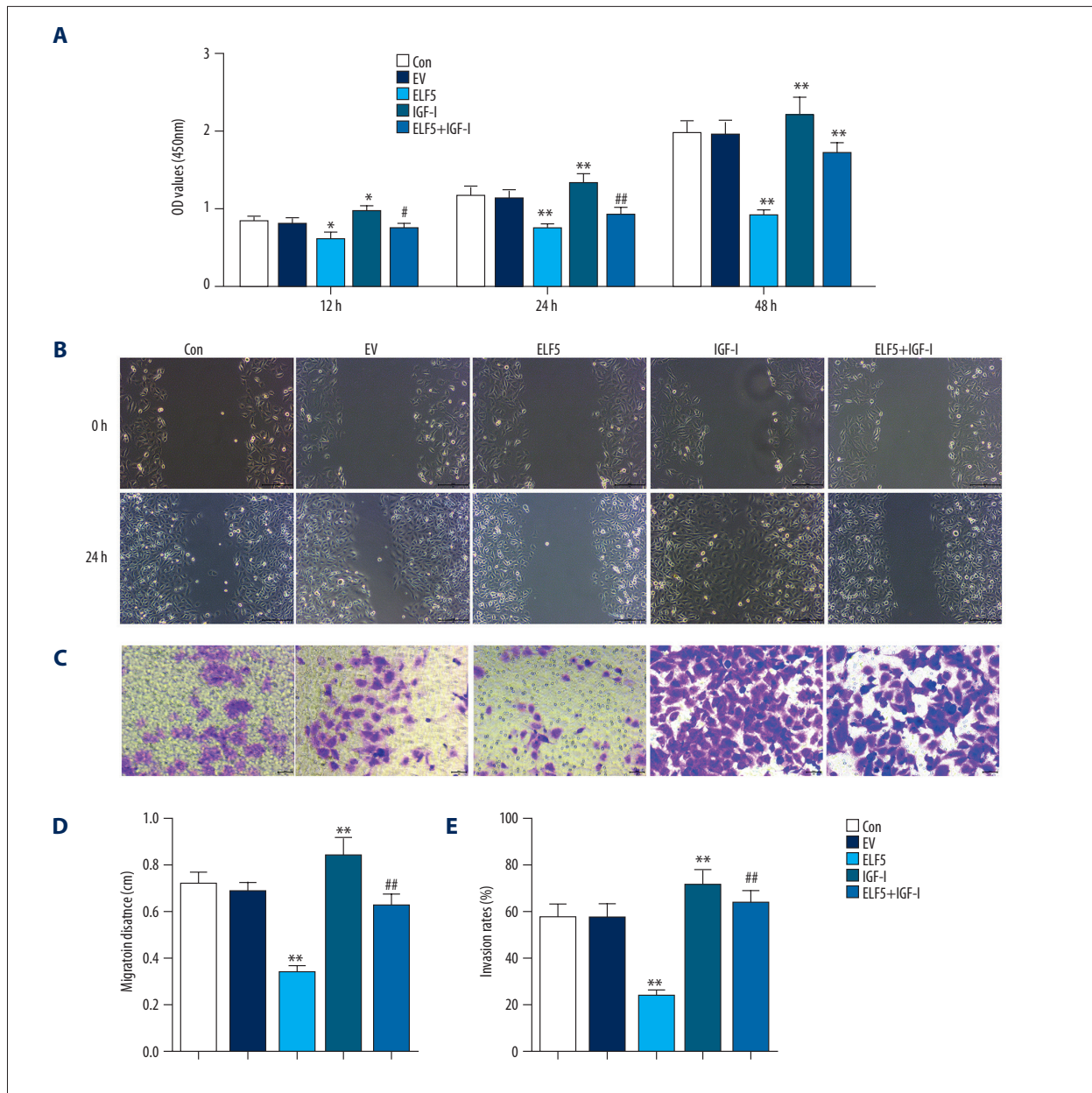


Figure 5. The inhibition of E74-like factor 5 (ELF5) on invasion, migration and cell viability were enhanced by IGF-I. **(A)** The viability of cells was detected by cell counting kit (CCK-8). **(B)** The wound assay was used to perform the migration. **(C)** The Transwell assay was used to test the invasion. **(D, E)** The percent migration and invasion rate in SKOV-5 cells was expressed as a percentage of control. All data were shown as means \pm SEM. * $P < 0.05$, ** $P < 0.01$, vs. control. # $P < 0.05$, ## $P < 0.01$, vs. ELF5.

The ELF5 gene promoted apoptosis of ovarian cancer SKOV3 cells. These experimental results are consistent with the results of clinical pathology experimental data [19]. VEGF is an important molecule in ovarian cancer, and its expression is negatively correlated with prognosis [28]. Ovarian cancer angiogenesis has been widely reported [29]. However, the role of ELF5 in ovarian cancer angiogenesis is not fully understood. Therefore, we performed an *in vitro* angiogenesis experiment to detect angiogenesis. We discovered that angiogenesis in

ovarian cancer SKOV3 cells was significantly reduced after ELF5 gene transfection. Western blot analysis data showed that VEGF was downregulated after ELF5 gene transfection. These findings suggested that ELF5 gene can inhibit ovarian cancer angiogenesis, at least in SKOV3 cells.

Invasive ability *in vitro* is important in determining tumor metastasis potential [30]. Wound-healing assay and Transwell chamber analysis data showed that the metastasis ability of

ovarian cancer SKOV3 cells was significantly decreased after transfection of the ELF5 gene, indicating that the ELF5 gene has a significant inhibitory effect on host invasion and motility of ovarian cancer SKOV3 cells. Studies have shown that epithelial-mesenchymal cells play a vital role in tumor invasion and metastasis [31]. Protein E-cadherin, which is mainly regulated by the transcription factor Snail, is one of the most important EMT markers [32]. Snail binds to the E-cadherin promoter and inhibits the transcription of E-cadherin. Significant upregulation of protein and fibronectin is the hallmark of EMT [33]. ELF5 can reduce the invasiveness of breast cancer cells and inhibit EMT by directly inhibiting the expression of Snail [34]. Therefore, differences in EMT markers, including the expression of E-cadherin, N-cadherin, and Snail, were detected by qPCR and Western blot. The results revealed that the expressions of N-cadherin and Snail in the ELF5 group were significantly lower than those in the control and EV groups, whereas the expression of E-cadherin was significantly higher in the ELF5 group than in the control and EV groups. These results indicated that ELF5 plays a vital role in development of ovarian cancer, at least in SKOV3 cancer cells line.

Kaye reported high expression of the P13K/AKT signaling pathway in ovarian cancer [35]. The P13K/AKT pathway can induce the development of tumor and promote metastasis of tumor via various pathways [36]. Similar to other studies [37,38], we discovered that the phosphorylation protein levels of AKT and P13K were significantly increased on SKOV3 cells, which were

reversed by transfected ELF5, suggesting that the P13K/AKT signaling pathway may be closely correlated to the development of ovarian cancer. Subsequently, the P13K/AKT signaling pathway inhibitor-IGF-I was used to treat SKOV3 cells, and we found that treatment with IGF-I reversed the effect of ELF5 by increasing viability, invasion, and migration of the cells. These findings suggest that activation of the P13K/AKT signaling pathway facilitated the progression of ovarian cancer. However, the potential role of ELF5 in ovarian cancer cells still remains unclear, and the involvement of other signaling pathways in the regulation of ovarian cancer by ELF5 should be investigated.

Conclusions

In this study, we discovered that ELF5 was downregulated in ovarian cancer cell lines, and this phenomenon was associated with ovarian cancer aggressiveness. Overexpression of ELF5 induced by transfection was observed to inhibit cell growth, metastasis, and phosphorylation protein levels of AKT and P13K. Furthermore, IGF-1 impaired the inhibitory effects of ELF5 on the malignant phenotypes of SKOV3 cells. These data provided an important theoretical basis for clinical treatment of ovarian cancer.

Conflict of interest

None.

References:

- Suh DH, Kim MK, Kim HS et al: Epigenetic therapies as a promising strategy for overcoming chemoresistance in epithelial ovarian cancer. *J Cancer Prev*, 2013; 18(3): 227–34
- Muralidhar GG, Barbolina MV: Chemokine receptors in epithelial ovarian cancer. *Int J Mo Sci*, 2013; 15(1): 361–76
- Huhtaniemi I, Hovatta O, La Marca A et al: Advances in the molecular pathophysiology, genetics, and treatment of primary ovarian insufficiency. *Trends Endocrinol Metab*, 2018; 29(6): 400–19
- Giornelli GH: Management of relapsed ovarian cancer: A review. *Springer Plus*, 2016; 5(1): 1197
- Pylvas-Eerola M, Liakka A, Puistola U et al: Cancer stem cell properties as factors predictive of chemoresistance in neoadjuvantly-treated patients with ovarian cancer. *Anticancer Res*, 2016; 36(7): 3425–31
- Zhou J, Chehab R, Tkalcovic J et al: Elf5 is essential for early embryogenesis and mammary gland development during pregnancy and lactation. *EMBO J*, 2005; 24(3): 635–44
- Mallepell S, Krust A, Chambon P, Briskin C: Paracrine signaling through the epithelial estrogen receptor alpha is required for proliferation and morphogenesis in the mammary gland. *Proc Natl Acad Sci USA*, 2006; 103(7): 2196–201
- Schramek D, Leibbrandt A, Sigl V et al: Osteoclast differentiation factor RANKL controls development of progestin-driven mammary cancer. *Nature*, 2010; 468(7320): 98–102
- Luo D, Xu X, Li J et al: The PDK1/cJun pathway activated by TGFbeta induces EMT and promotes proliferation and invasion in human glioblastoma. *Int J Oncol*, 2018; 53(5): 2067–80
- Zuo Q, Wang J, Chen C et al: ASCL2 expression contributes to gastric tumor migration and invasion by downregulating miR223 and inducing EMT. *Mol Med Rep*, 2018; 18(4): 3751–59
- Rogers RL, Van Seuning I, Gould J et al: Transcript profiling of Elf5+/- mammary glands during pregnancy identifies novel targets of Elf5. *PLoS One*, 2010; 5(10): e13150
- Bader AG, Kang S, Zhao L, Vogt PK: Oncogenic PI3K deregulates transcription and translation. *Nat Rev Cancer*, 2005; 5(12): 921–29
- Zhang Z, Yao L, Yang J et al: PI3K/Akt and HIF1 signaling pathway in hypoxia-ischemia (Review). *Mol Med Rep*, 2018; 18(4): 3547–54
- Cantley LC: The phosphoinositide 3-kinase pathway. *Science (New York, NY)*, 2002; 296(5573): 1655–57
- Bhat SA, Mir MUR, Majid S et al: Diagnostic utility of glycosyltransferase mRNA expression in gastric cancer. *Hematol Oncol Stem Cell Ther*, 2018; 11(3): 158–68
- Wu D, Lu P, Mi X, Miao J: Downregulation of miR-503 contributes to the development of drug resistance in ovarian cancer by targeting PI3K p85. *Arch Gynecol Obstet*, 2018; 297(3): 699–707
- Kim S, Lee Y, Lee S, Kim T: Ovarian tissue cryopreservation and transplantation in patients with cancer. *Obstet Gynecol Sci*, 2018; 61(4): 431–42
- Torre LA, Bray F, Siegel RL et al: Global cancer statistics, 2012. *Cancer J Clin*, 2015; 65(2): 87–108
- Yan H, Qiu L, Xie X et al: ELF5 in epithelial ovarian carcinoma tissues and biological behavior in ovarian carcinoma cells. *Oncol Rep*, 2017; 37(3): 1412–18
- Yan H, Sun Y: Evaluation of the mechanism of epithelial-mesenchymal transition in human ovarian cancer stem cells transfected with a WW domain-containing oxidoreductase gene. *Oncol Lett*, 2014; 8(1): 426–30
- Ismail S, Haris K, Abdul Ghani AR et al: Enhanced induction of cell cycle arrest and apoptosis via the mitochondrial membrane potential disruption in human U87 malignant glioma cells by aloe emodin. *J Asian Nat Prod Res*, 2013; 15(9): 1003–12

22. Zhang K, Shen Z, Liang X et al: Down-regulation of GPR137 expression inhibits proliferation of colon cancer cells. *Acta Biochim Biophys Sin*, 2014; 46(11): 935–41
23. Tang YC, Yuwen H, Wang K et al: Aneuploid cell survival relies upon sphingolipid homeostasis. *Cancer Res*, 2017; 77(19): 5272–86
24. Kharroubi Lakouas D, Huglo D, Mordon S, Vermandel M: Nuclear medicine for photodynamic therapy in cancer: Planning, monitoring and nuclear PDT. *Photodiagnosis Photodyn Ther*, 2017; 18: 236–43
25. Liu N, Yang HL, Wang P et al: Functional proteomic analysis reveals that the ethanol extract of *Annona muricata* L. induces liver cancer cell apoptosis through endoplasmic reticulum stress pathway. *J Ethnopharmacol*, 2016; 189: 210–17
26. Kwon SB, Kim MJ, Yang JM et al: *Cudrania tricuspidata* stem extract induces apoptosis via the extrinsic pathway in SiHa cervical cancer cells. *PLoS One*, 2016; 11(3): e0150235
27. Simoes VL, Alves MG, Martins AD et al: Regulation of apoptotic signaling pathways by 5 α -dihydrotestosterone and 17 β -estradiol in immature rat Sertoli cells. *J Steroid Biochem Mol Biol*, 2013; 135: 15–23
28. Chen Y, Zhang L, Liu WX, Wang K: VEGF and SEMA4D have synergistic effects on the promotion of angiogenesis in epithelial ovarian cancer. *Cell Mol Biol Lett*, 2018; 23: 2
29. Nwani NG, Sima LE, Nieves-Neira W, Matei D: Targeting the microenvironment in high grade serous ovarian cancer. *Cancers (Basel)*, 2018; 10(8): pii: E266
30. Collins RJ, Morgan LD, Owen S et al: Mechanistic insights of epithelial protein lost in neoplasm in prostate cancer metastasis. *Int J Cancer*, 2018; 143(10): 2537–50
31. Shen Z, Zhu D, Liu J et al: 27-Hydroxycholesterol induces invasion and migration of breast cancer cells by increasing MMP9 and generating EMT through activation of STAT-3. *Environ Toxicol Pharmacol*, 2017; 51: 1–8
32. Harada K, Sato Y, Ikeda H et al: Epithelial-mesenchymal transition induced by biliary innate immunity contributes to the sclerosing cholangiopathy of biliary atresia. *J Pathol*, 2009; 217(5): 654–64
33. Scheel C, Weinberg RA: Cancer stem cells and epithelial-mesenchymal transition: Concepts and molecular links. *Semin Cancer Biol*, 2012; 22(5–6): 396–403
34. Chakrabarti R, Hwang J, Andres Blanco M et al: Elf5 inhibits the epithelial-mesenchymal transition in mammary gland development and breast cancer metastasis by transcriptionally repressing Snail2. *Nat Cell Biol*, 2012; 14(11): 1212–22
35. Kaye SB: Progress in the treatment of ovarian cancer-lessons from homologous recombination deficiency-the first 10 years. *Ann Oncol*, 2016; 27(Suppl. 1): i1–i3
36. Xu J, Li Z, Su Q et al: TRIM29 promotes progression of thyroid carcinoma via activating P13K/AKT signaling pathway. *Oncol Rep*, 2017; 37(3): 1555–64
37. Papa A, Caruso D, Strudel M et al: Update on Poly-ADP-ribose polymerase inhibition for ovarian cancer treatment. *J Transl Med*, 2016; 14: 267
38. Tan N, Zheng H, Huang JJ et al: [Effect of P13K/AKT signal pathway regulation on expression of XIAP and cIAP2 in ovarian cancer cells]. *Zhonghua Bing Li Xue Za Zhi*, 2013; 42(9): 613–14 [in Chinese]